ORIGINAL RESEARCH

E. Matsusue
S. Fujii
Y. Kanasaki
T. Kaminou
E. Ohama
T. Ogawa

Cerebellar Lesions in Multiple System Atrophy: Postmortem MR Imaging—Pathologic Correlations

BACKGROUND AND PURPOSE: Cerebellar atrophy and white matter T2-hyperintensities have been characterized as cerebellar lesions of multiple system atrophy (MSA). The aim of the study was to correlate MR images with histologic findings in cerebellar lesions of MSA.

MATERIALS AND METHODS: Postmortem T2-weighted images using 1.5T were compared with histologic findings in 7 postmortem-proved cases with MSA. The MR imaging findings in the cerebellar cortices and deep white matter dentate nucleus regions were compared with their histologic findings in each case.

RESULTS: We detected 3 types of cerebellar changes: type 1, no apparent atrophy or signal-intensity changes; type 2, cerebellar atrophy and inhomogeneous (patchy and/or confluent) cerebellar white matter hyperintensities; and type 3, cerebellar atrophy and diffuse white matter hyperintensities. Hypointensities were seen in the dentate nucleus regions. Atrophy of the cerebellar white matter was more severe than that of cerebellar cortices, and this anatomy was well depicted on coronal images. Histologically, degeneration was more severe in the cerebellar white matter than in the cerebellar cortices. Hyperintensities in the cerebellar white matter showed loss of myelinated fibers and gliosis. Hypointensities in the dentate nucleus regions revealed diffuse ferritin deposition in preserved dentate nuclei and white matter both around and within the nuclei.

CONCLUSIONS: Hyperintensities in the cerebellar white matter reflect degenerated white matter associated with loss of myelinated fibers and gliosis, whereas hypointensities in the dentate nucleus regions reflect diffuse ferritin deposition in preserved dentate nuclei and white matter around and within the nuclei. Degeneration is more severe in the cerebellar white matter than in the cerebellar cortices.

Multiple system atrophy (MSA) is a sporadic adult-onset progressive neurodegenerative disorder, characterized pathologically by degeneration of the basal ganglia and the olivopontocerebellar system and clinically known as parkinsonism, cerebellar ataxia, and autonomic dysfunction. MSA has 3 subtypes: olivopontocerebellar atrophy (OPCA), striatonigral degeneration (SND), and Shy-Drager syndrome. Also, sporadic OPCA, SND, and Shy-Drager syndrome can all mutually exist both pathologically and clinically. The common and specific histologic findings in MSA are glial cytoplasmic inclusions (GCIs).[1,2] The major constituent of GCIs is α-synuclein, which is also a major component of the Lewy body, which is the pathologic hallmark lesion in Parkinson disease and dementia with Lewy bodies. Recently the term "synucleinopathy" has been proposed to encompass a presumed common pathogenic process shared by these neurodegenerative disorders.[3,4]

On the basis of symptoms at onset, MSA has been divided into 2 forms: MSA-C, characterized by a predominance of cerebellar symptoms; and MSA-P, in which parkinsonism is prevalent.[5,6] Hyperintensities in the pons, middle cerebellar peduncles, and cerebellum, corresponding to pontocerebellar tract atrophy and hyper- and/or hypointensities associated with posterior putaminal atrophy on T2-weighted images, have been described as characteristic findings on MR images in patients with MSA.[7-12]

Diffusion-weighted MR imaging (DWI) has emerged as a useful method for detecting early pathologic changes of various diseases based on water diffusivity.[13] Apparent diffusion coefficient (ADC) and fractional anisotropy (FA) values have been used to evaluate the degree of tissue degeneration in various disorders. Recent evidence has demonstrated that ADC values in the pons, cerebellum, and putamen are significantly higher,[14-16] whereas FA values are lower in MSA than in Parkinson disease or controls.[14,17] This difference suggests that DWI may be a useful tool in the diagnosis of MSA.

There have been several reports studying the correlation of antemortem MR images with histologic findings[7-9] in cerebellar lesions of MSA. However, there have been no reports directly correlating postmortem MR images with histologic findings in cerebellar lesions. Our aim was to elucidate MR imaging—pathologic correlations on postmortem T2-weighted images and their histologic findings in 7 autopsy-proved cases of cerebellar lesions of MSA.

Materials and Methods

We retrospectively analyzed brain MR images in 7 postmortem-proved MSA cases (5 women, 2 men; mean age, 71 years; age range, 55–83 years) and, with the consent of relatives, were able to conduct postmortem examination on the brains of the deceased. As for the histologic diagnosis of MSA, established MSA neuropathologic criteria were applied, checking the presence of GCIs with neuronal loss and gliosis in a number of structures including the putamen, substantia nigra, locus coeruleus, basis pontis, inferior olivary nucleus, and dorsal motor nucleus of the vagus.[18] The GCIs were examined by using α-synuclein immunohistochemistry. Histologic findings also

Received February 19, 2009; accepted after revision April 6.

From the Division of Radiology (E.M., S.F., Y.K., T.K., T.O.), Department of Pathophysiological and Therapeutic Science, Faculty of Medicine, Tottori University, Yonago, Tottori, Japan; and Department of Neuropathology (E.O.), Institute of Neurological Sciences, Faculty of Medicine, Tottori University, Yonago, Tottori, Japan.

Please address correspondence to Eiji Matsusue, MD, Division of Radiology, Department of Pathophysiological and Therapeutic Science, Faculty of Medicine, Tottori University. 36-1 Nishi-cho, Yonago, Tottori 683-8504, Japan; e-mail: matsusue@grape.med.tottori-u.ac.jp

DOI 10.3174/ajnr.A1662

indicated 5 cases of OPCA, 1 case of SND, and 1 case of combined OPCA and SND.

T2-weighted images of 10% formalin-fixed brains at postmortem examination (postmortem MR images) were obtained in all cases by using a 1.5T imaging system (Symphony; Siemens, Erlangen, Germany). First, we washed the fixed brains by using running tap water for 24 consecutive hours. Each brain was then put into its original box, which was void of water. Therefore, the fixed brains were completely surrounded by air with the exception of some residual water in the ventricles and sulci. The fixed brains in the box were positioned in a standard way in the 8-channel head coil, and axial and coronal fast spin-echo T2-weighted images (TR/TE, 4000/81; 320 × 512 matrix; 150-mm FOV; section 4/1 mm) were obtained. For gross examination, each cerebellum was cut into 3-mm-thick coronal sections, each cerebrum was cut into 5-mm-thick coronal sections, and each brain stem had 3-mm-thick axial sections. Therefore, sagittal MR images were not obtained because each brain was not cut into sagittal sections for gross examination.

Evaluation of antemortem MR images was not performed because all cases belonged to other hospitals and the MR images were available for only 3 cases. However, the findings at postmortem T2-weighted imaging were qualitatively well correlated with the in vivo imaging findings, despite the shortening of T1 and T2 relaxation times secondary to formalin fixation.[19]

For MR-pathologic direct correlation, neuropathologic examinations were performed in all cases by using 5 staining methods: hematoxylin-eosin, Bielschowsky, Klüver-Barrera, glial fibrillary acidic protein (GFAP), and ferritin immunohistochemistry. The Bielschowsky method was used to evaluate axons, and the Klüver-Barrera method was used to evaluate myelin. GFAP immunohistochemistry was used to evaluate gliosis, and ferritin immunohistochemistry was used to reveal ferritin deposits.

Evaluation of Postmortem MR Imaging Findings

The presence of atrophy and signal-intensity change of cerebellar cortices, deep white matter and dentate nucleus regions was evaluated on postmortem coronal T2-weighted images. Cerebellar cortices were considered to be atrophied if there were dilations of folial fissures of the cerebellum. Cerebellar deep white matter was considered to be atrophied if there were loss of volume and a concaved contour of the white matter. To appreciate the increased signal intensity of the cerebellar deep white matter, signal-intensity changes of cerebellar white matter were compared with those of cerebral white matter on coronal images. The extent of T2 hyperintensities of the cerebellar white matter was graded as follows: none, inhomogeneous (presence of patchy and/or confluent hyperintense areas), and diffuse. Dentate nuclei were considered to be atrophied if they had a flattened appearance.

We also evaluated whether axial images were useful for the detection of cerebellar cortices, deep white matter, and dentate nuclei. The presence of atrophy and signal-intensity change of the pons and middle cerebellar peduncles was evaluated on postmortem axial T2-weighted images. In our final analysis, we evaluated cerebellar symptoms and measured the duration of the disease for each case.

Postmortem MR Imaging and Pathologic Correlations

The MR imaging findings in the cerebellum were compared with their histologic findings in each case. The following cerebellar regions were histologically assessed for the correlations: 1) cerebellar cortices, 2) deep cerebellar white matter, and 3) dentate nucleus regions.

Results

Postmortem MR Imaging Findings

There were 3 types of cerebellar changes on postmortem coronal T2-weighted MR images: type 1, no apparent cerebellar atrophy or signal-intensity changes (case 1) (Fig 1*A*, -*B*); type 2, atrophy of cerebellar cortices and deep white matter and inhomogeneous (patchy and/or confluent) cerebellar deep white matter hyperintensities (cases 2–4) (Fig 2*A*, -*B*); and type 3, atrophy of cerebellar cortices and white matter and diffuse cerebellar deep white matter hyperintensities (cases 5–7) (Fig 3*A*, -*B*). The atrophy of cerebellar deep white matter and cortices was equally apparent in both types 2 and 3. However, the atrophy was more severe in cerebellar white matter than in cerebellar cortices in types 2 and 3. Diffuse hypointensities were seen in the dentate nucleus region in all types. Atrophy was not seen in types 1 and 2 but was present in type 3. Also, hypointensities of the dentate nucleus region were conspicuous due to diffuse hyperintensities of cerebellar white matter in type 3. In all cases, cerebellar white matter and cortices and dentate nucleus regions were not precisely depicted on axial images, especially in types 2 and 3 (Figs 1*A*, 2*A*, and 3*A*). As to changes of the middle cerebellar peduncle and pontine base, no signal-intensity change or atrophy was seen in type 1. In types 2 and 3, there were diffuse hyperintensities with atrophy in middle cerebellar peduncles and crossed hyperintensities in the atrophied pontine base. More severe atrophy and increased signal intensities were seen in type 3 than in type 2.

Cerebellar symptoms such as ataxic gait, dysarthria, or nystagmus were observed in types 2 and 3, but not in type 1. The total duration of illness in all our cases was as follows: type 1, 5 years (case 1); type 2, 6 years (cases 3 and 4) and 7 years (case 2); type 3, 8 years (cases 5 and 6) and 13 years (case 7). Among the examined, case 1 (type 1) had the shortest duration of illness (5 years) and case 7 had the longest duration of illness (13 years).

Postmortem MR Imaging and Pathologic Correlations

In the case of type 1, cerebellar cortices without atrophy showed histologically well preserved neurons without apparent gliosis. Cerebellar white matter without signal-intensity change or atrophy (Fig 1*B*) showed histologically mild loss of myelin and axons with mild gliosis (Fig 2*C–E*). Hypointensities in the dentate nucleus regions (Fig 1*B*) reflected diffuse ferritin deposition and well-preserved dentate nuclei and white matter around and within the nuclei (Figs 2*C*, -*F*). Histologically, the case was diagnosed as SND type (case 1).

In all cases of type 2, inhomogeneous (patchy and/or confluent) deep cerebellar white matter hyperintensities with atrophy (Fig 2*B*) showed loss of myelin and axons with gliosis but no tissue rarefaction (Fig 3*C–E*). The atrophy was more severe in the cerebellar white matter compared with cerebellar cortices (Fig 2*B*). Hypointensities in the dentate nucleus regions (Fig 2*B*) showed well-preserved dentate nuclei and white matter within and surrounding the dentate nuclei and diffuse ferritin deposition (Figs 2*C*, -*F*). Histologically, they were diagnosed as SND plus OPCA type (case 2) and OPCA type (cases 3 and 4), respectively.

In all cases of type 3, diffuse cerebellar white matter hyper-

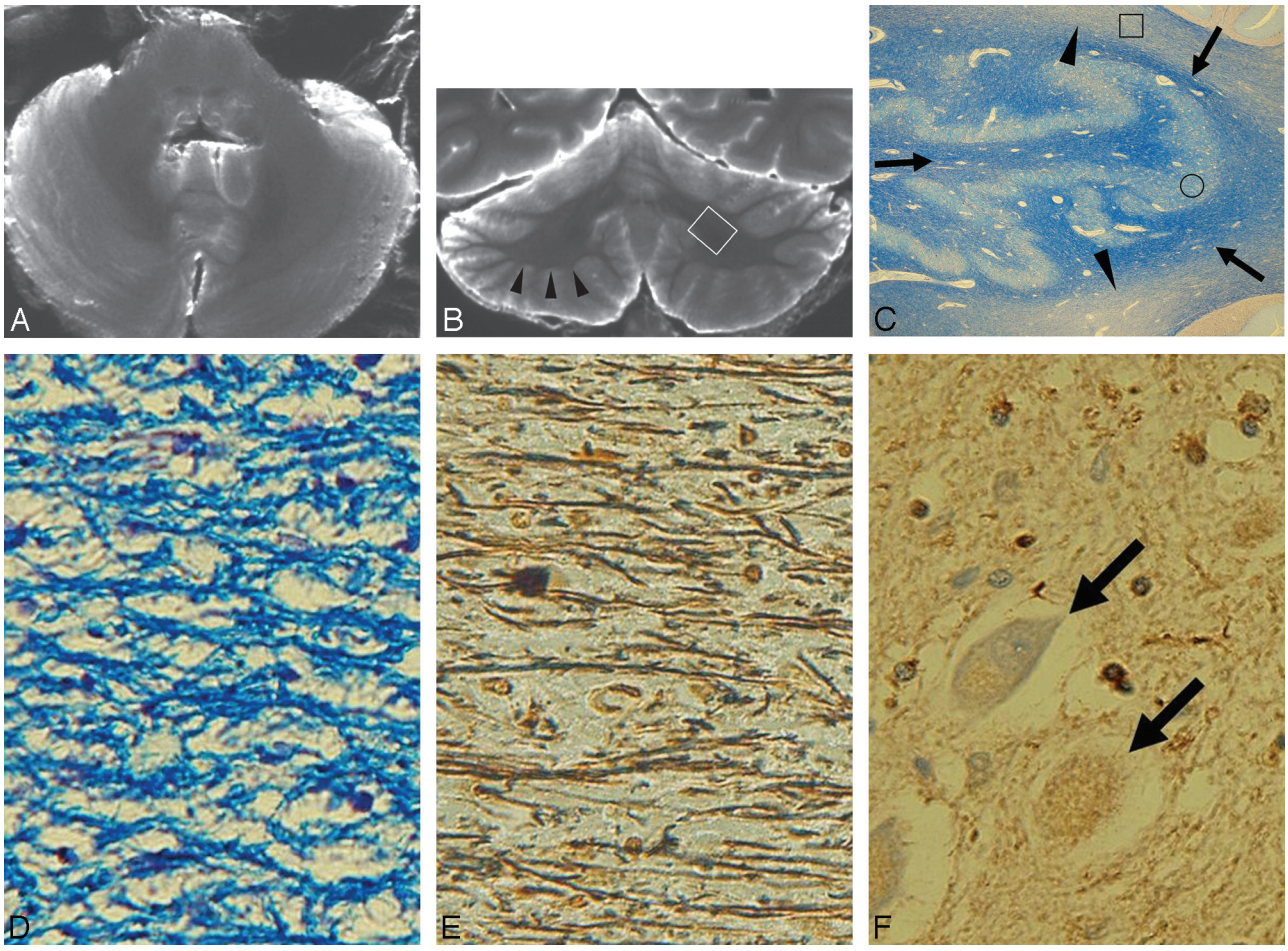

Fig 1. Case 1 (type 1). *A* and *B*, Postmortem axial (*A*) and coronal (*B*) T2-weighted images show no apparent cerebellar atrophy or signal-intensity changes. Note the convex contour of the cerebellar deep white matter on the coronal image (*arrowheads* in *B*). No signal-intensity changes or atrophy is seen in the middle cerebellar peduncles or pontine base. Hypointensities are seen in the dentate nucleus regions. Cerebellar cortices, deep white matter, and dentate nucleus regions are depicted well on the coronal image (*B*) compared with the axial image (*A*). *C*, A myelin-stained section corresponding to the white boxed area in *B* shows mild pallor in the deep cerebellar white matter (*arrowheads*). Dentate nucleus and white matter within and surrounding the dentate nucleus are well preserved (*arrows*) (Klüver-Barrera stain, original magnification ×5). *D* and *E*, Histologic finding of the boxed area in *C* shows mild loss of myelin (*D*) and axons (*E*) with mild gliosis (Klüver-Barrera stain, original magnification ×200, *D*; Bielschowsky stain, original magnification ×200, *E*). *F*, Immunohistochemical findings of the dentate nucleus (circled area in *C*) show diffuse ferritin deposition and well-preserved neurons (*arrows*) (ferritin stain, original magnification ×200).

intensities with atrophy (Fig 3*B*) showed tissue rarefaction with loss of myelin and axons as well as gliosis (Fig 3*C–E*). Atrophy was seen in both cerebellar white matter and cortices but was more severe in the cerebellar white matter compared with the cerebellar cortices (Figs 3*B*). Atrophied and hypointense dentate nucleus regions (Fig 3*B*) showed atrophied but well-preserved neurons with gliosis and loss of myelin and axons of white matter within and surrounding the nuclei and diffuse ferritin deposition (Figs 3*C, -F*). Histologically, all cases were diagnosed as OPCA type (cases 5–7).

Discussion

Pathologic Distribution of the Olivopontocerebellar Region in MSA

In MSA, the olivopontocerebellar system is usually involved.[20] Input cerebellar fibers, including pontocerebellar fibers (transverse pontine and middle cerebellar peduncle) and olivocerebellar fibers (inferior cerebellar peduncle), are mainly affected. In our cases with hyperintensities and atrophy in the deep cerebellar white matter (types 2 and 3), there were diffuse hyperintensities with atrophy in middle cerebellar peduncles and crossed hyperintensities in the atrophied pontine base. Also, more severe atrophy and increased signal intensities were seen in cases with diffuse hyperintensity of the cerebellar white matter (type 3) than in cases with inhomogeneous hyperintensity of cerebellar white matter (type 2). These findings suggest that the degree of pontocerebellar fiber degeneration is correlated with that of cerebellar white matter degeneration.

As to output cerebellar fibers, the fibers projecting from Purkinje cells to the dentate nuclei are affected in variable degrees, yet dentatorubral fibers (superior cerebellar peduncle) are well preserved.

Signal-Intensity Change and Atrophy of the Cerebellum

Mizutani[21] reported that in patients with MSA, cerebellar white matter is usually more affected than cerebellar cortices. Our MR images indicated that in cases with cerebellar white matter hyperintensities with atrophy (types 2 and 3), the atrophy was more severe in the cerebellar white matter compared with the cerebellar cortices. In addition, the degeneration was histologically more severe in the white matter compared with

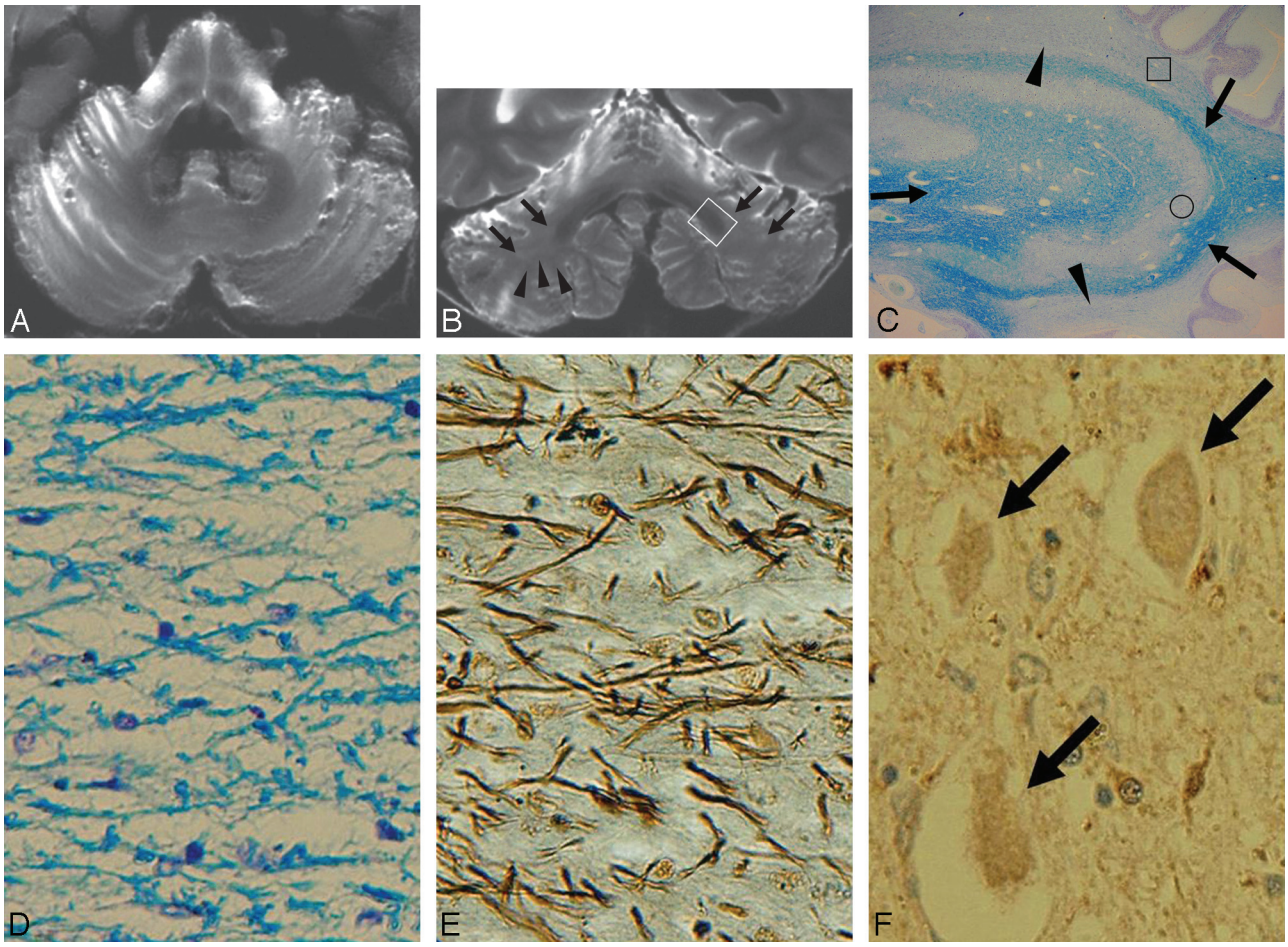

Fig 2. Case 2 (type 2). *A* and *B*, Postmortem axial (*A*) and coronal (*B*) T2-weighted images show atrophied cerebellar cortices with dilation of folial fissures and atrophied deep cerebellar white matter with a concave contour (*arrowheads* in *B*). Note the confluent hyperintensities in the cerebellar deep white matter (*arrows* in *B*). Hypointensities are seen in the dentate nucleus regions (*A* and *B*). There are diffuse hyperintensities and atrophy in the middle cerebellar peduncles and crossed hyperintensities and atrophy in the pontine base (*A*). Cerebellar deep white matter and dentate nucleus regions are not depicted precisely on the axial image (*A*), due to partial volume effects of water seen in dilated folial fissures. *C*, A myelin-stained section corresponding to the white boxed area in *B* shows pallor in the deep cerebellar white matter (*arrowheads*). Dentate nucleus and white matter within and surrounding the dentate nucleus are well preserved (*arrows*) (Klüver-Barrera stain, original magnification ×5). *D* and *E*, Histologic finding of the boxed area in *C* shows loss of myelin (*D*) and axons (*E*) with gliosis (Klüver-Barrera stain, original magnification ×200, *D*,. Bielschowsky stain, original magnification ×200, *E*). *F*, Immunohistochemical finding of the dentate nucleus (circled area in *C*) shows diffuse ferritin deposition and well-preserved neurons (*arrows*) (ferritin stain, original magnification ×200).

the cortices. Even in the case without cerebellar atrophy or signal-intensity changes (type 1), cerebellar white matter showed histologically mild degeneration, including loss of myelin and axons with mild gliosis. All of these findings are consistent with predominant cerebellar white matter involvement in MSA.

Histologic findings also indicated that hyperintensities of cerebellar white matter showed loss of myelin and axons with gliosis, which reflected histologic changes in MSA. Also, diffuse cerebellar white matter hyperintensities seen in type 3 showed tissue rarefaction with severe loss of myelin and axons as well as gliosis. Severe tissue rarefaction in cerebellar white matter is sometimes seen in cases with MSA.[21]

As for duration of illness, more severe atrophy and increased signal intensities, suggesting more severe degeneration, were seen in cerebellar white matter as well as cerebellar cortices in our cases with a longer duration of illness.

Change of the Dentate Nucleus

In MSA, dentate nuclei are preserved, as well as their projections to the red nuclei and the thalami through the superior cerebellar peduncles. As to signal intensity of the dentate nuclei on T2-weighted imaging, it decreases in proportion to ferritin concentration of the nuclei and becomes more prominent with age.[22]

In types 1 and 2, T2-weighted images showed diffuse hypointensities of dentate nucleus regions with their preserved volume. Ferritin deposition of the dentate nucleus regions was diffuse in all cases. Even in type 3 with diffuse cerebellar white matter hyperintensities, the degeneration of the dentate nuclei and white matter both within and surrounding the nuclei was mild. Furthermore, neurons of the nuclei were well preserved.

Consequently, signal-intensity change of the dentate nucleus region in our cases was considered as a reflection of diffuse ferritin deposition in the preserved dentate nucleus and white matter both within and surrounding the nucleus, seeming to reflect age-related change. Also, in type 3, hypointensities of the dentate nucleus region were conspicuous due to diffuse hyperintensities of cerebellar white matter, showing the severe degeneration of MSA.

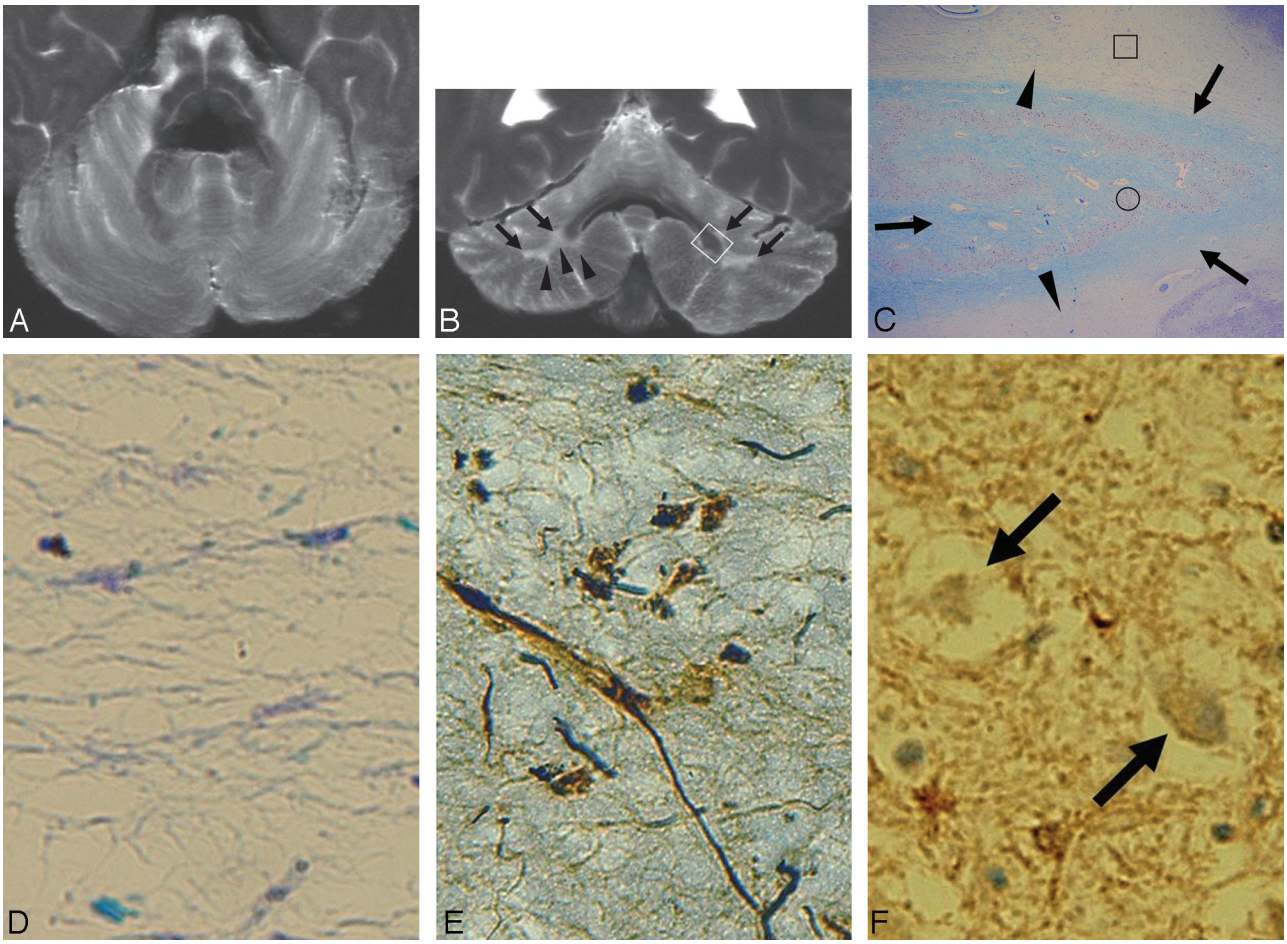

Fig 3. Case 5 (type 3). *A* and *B*, Postmortem axial (*A*) and coronal (*B*) T2-weighted images show atrophied cerebellar cortices with dilation of folial fissures and atrophied deep cerebellar white matter with a concave contour (*arrowheads* in *B*). Note the diffuse hyperintensities in the deep cerebellar white matter (*arrows* in *B*). There are diffuse hyperintensities and atrophy in the middle cerebellar peduncles and crossed hyperintensities and atrophy in the pontine base (*A*). Cerebellar deep white matter and dentate nucleus regions are not depicted precisely on the axial image (*A*). Hypointensities of the dentate nucleus region are conspicuous due to diffuse hyperintensities of the cerebellar deep white matter (*B*). *C*, A myelin-stained section corresponding to the white boxed area in *B* shows the diffuse pallor of the deep cerebellar white matter (*arrowheads*). Mild atrophy of the dentate nucleus and mild pallor of the white matter within and surrounding the dentate nucleus are seen (*arrows*) (Klüver-Barrera stain, original magnification ×5). *D* and *E*, Histologic findings of the boxed area in *C* show tissue rarefaction associated with loss of myelin (*D*) and axons (*E*) as well as gliosis (Klüver-Barrera stain, original magnification ×200, *D*; Bielschowsky stain, original magnification ×200, *E*). *F*, Immunohistochemical findings of the dentate nucleus (circled area in C) show diffuse ferritin deposition and preserved neurons with atrophy (*arrows*) (ferritin stain, original magnification ×200).

Usefulness of the Coronal Image

In all of our cases, cerebellar cortices, deep white matter, and dentate nucleus regions were well depicted on coronal images compared with axial ones. Coronal images were also useful to evaluate signal-intensity changes of cerebellar white matter precisely. Depicting cerebellar white matter and cortices and dentate nucleus regions, especially in cases with cerebellar atrophy, is susceptible to the partial volume effects with cerebellar folia on axial images. Coronal images can precisely demonstrate those cerebellar anatomies without the partial volume effect with cerebellar folia, especially in the cases with severe cerebellar atrophy.

In the past, axial images were commonly used to evaluate cerebellar white matter in MSA; however, signal-intensity change and/or atrophy of cerebellar white matter on axial images may not have been depicted in the early stage of MSA due to partial volume effects of cerebellar folia. Therefore, coronal images, including conventional MR imaging and physiologic MR imaging such as DWI, may be useful to detect signal-intensity change and/or atrophy of cerebellar white matter in the early stages of MSA. To further clarify the diagnostic value of using coronal images in MSA, one would need to perform a prospective MR imaging study comparing the cerebellar lesions that have MSA with age-matched controls on a larger pool of subjects, by using axial and coronal MR imaging.

Conclusions

Postmortem coronal T2-weighted images revealed that atrophy was more severe in cerebellar white matter compared with cerebellar cortices in cases with MSA. Hyperintensities in the cerebellar white matter reflected degenerated white matter associated with loss of myelinated fibers and gliosis, whereas hypointensities in the dentate nucleus regions reflected preserved dentate nuclei and white matter both within and surrounding the nuclei. These findings reflected characteristic histologic findings of cerebellar lesions in MSA. The coronal images were useful in exactly depicting the location of cerebellar cortices and white matter as well as precisely detecting the location of dentate nucleus regions.

References

1. Papp MI, Kahn JE, Lantos PL, et al. **Glial cytoplasmic inclusions in the CNS of patients with multiple system atrophy (striatonigral degeneration, olivopontocerebellar atrophy and Shy-Drager syndrome).** *J Neurol Sci* 1989;94:79–100
2. Dickson DW, Lin W, Liu WK, et al. **Multiple system atrophy: a sporadic synucleinopathy.** *Brain Pathol* 1999;9:721–32
3. Spillantini MG, Crowther RA, Jakes R, et al. **Filamentous alpha-synuclein inclusions link multiple system atrophy with Parkinson's disease and dementia with Lewy bodies.** *Neurosci Lett* 1998;251:205–08
4. Galvin JE, Lee VMY, Trojanowski JQ. **Synucleinopathies: clinical and pathological implications.** *Arch Neurol* 2001;58:186–90
5. Wenning GK, Ben Shlomo Y, Magalhaes M, et al. **Clinical features and natural history of multiple system atrophy: an analysis of 100 cases.** *Brain* 1994;117:835–45
6. Gilman S, Low P, Quinn N, et al. **Consensus statement on the diagnosis of multiple system atrophy.** *Clin Auton Res* 1998;8:359–62
7. Savoiardo M, Strada L, Girotti F, et al. **Olivopontocerebellar atrophy: MR diagnosis and relationship to multisystem atrophy.** *Radiology* 1990;174:693–96
8. Yagishita A. **MR-pathologic correlations of pontocerebellar lesion in multiple system atrophy.** *Pathol and Clin Med (Japanese)* 1994;12:225–30
9. Schrag A, Kingsley D, Phatouros C, et al. **Clinical usefulness of magnetic resonance imaging in multiple system atrophy.** *J Neurol Neurosurg Psychiatry* 1998;65:65–71
10. Yekhlef F, Ballan G, Macia F, et al. **Differentiation of atypical parkinsonian syndromes with routine MRI.** *Neurology* 2000;55:1239–40
11. Bhattacharya K, Saadia D, Eisenkraft B, et al. **Brain magnetic resonance imaging in multiple-system atrophy and Parkinson disease: a diagnostic algorithm.** *Arch Neurol* 2002;59:835–42
12. Yekhlef F, Ballan G, Macia F, et al. **Routine MRI for the differential diagnosis of Parkinson's disease, MSA, PSP, and CBD.** *J Neural Transm* 2003;110:151–69
13. Le Bihan D, Turner R, Douek P, et al. **Diffusion MR imaging: clinical applications**. *AJR Am J Roentgenol* 1992;159:591–99
14. Ito M, Watanabe H, Kawai Y, et al. **Usefulness of combined fractional anisotropy and apparent diffusion coefficient values for detection of involvement in multiple system atrophy.** *J Neurol Neurosurg Psychiatry* 2007;78:722–28
15. Schocke MF, Seppi K, Esterhammer R, et al. **Trace of diffusion tensor differentiates the Parkinson variant of multiple system atrophy and Parkinson's disease.** *Neuroimage* 2004;21:1443–51
16. Kanazawa M, Shimohata T, Terajima K, et al. **Quantitative evaluation of brainstem involvement in multiple system atrophy by diffusion-weighted MR imaging.** *J Neurol* 2004;251:1121–24
17. Shiga K, Yamada K, Yoshikawa K, et al. **Local tissue anisotropy decreases in cerebellopetal fibers and pyramidal tract in multiple system atrophy.** *J Neurol* 2005;252:589–96. Epub 2005 Apr 18
18. Lowe J, Lennox G, Leigh PN. **Disorders of movement and system degeneration.** In: Graham DI, Lantos PL, eds. *Greenfield's Neuropathology*. 6th ed. London, UK; Arnold; 1997:297–300
19. Blamire AM, Rowe JG, Styles P, et al. **Optimising imaging parameters for post mortem MR imaging of the human brain.** *Acta Radiol* 1999;40:593–97
20. Wenning GK, Tison F, Elliott L, et al. **Olivopontocerebellar pathology in multiple system atrophy.** *Mov Disord* 1996;11:157–62
21. Mizutani T. **Pathological issues of spinocerebellar degeneration.** *Clin Neurosci (Japanese)* 1993;11:618–25
22. Hallgren B, Sourander P. **The effect of age on the non-haemin iron in the human brain.** *J Neurochem* 1958;3:41–51